Responses of the $Fe(CN)_2(CO)$ Unit to Electronic Changes as Related to Its Role in [NiFe]Hydrogenase

Chia-Huei Lai, Way-Zen Lee, Matthew L. Miller, Joseph H. Reibenspies, Donald J. Darensbourg,* and Marcetta Y. Darensbourg*

Contribution from the Department of Chemistry, Texas A&M University, College Station, Texas 77842-3012

Received June 12, 1998

Abstract: The observation of nearly identical infrared spectra in the diatomic (2000 cm^{-1}) region of oxidized forms of [NiFe]hydrogenases, as isolated from *Chromatium vinosum* (Happe et al. *Nature* **1997**, *385*, 126) and *Desulfovibrio gigas* (Volbeda et al. *J. Am. Chem. Soc*. **1996**, *118*, 12989) and the anion $(\eta^5\text{-}C_5H_5)Fe(CN)_2(CO)^-$ (Darensbourg et al. *J. Am. Chem. Soc*. **1997**, *119*, 7903), including isotopic label shifts, has prompted further development of the organometallic model complex as a spectroscopic reference. The vibrational spectroscopy of the pyramidal $Fe(CN)_2(CO)$ unit found in the salts of $(\eta^5\text{-}C_5H_5)Fe(CN)_2(CO)^-$ and $(\eta^5\text{-}C_5Me_5)Fe(CN)_2(CO)^-$ is thoroughly investigated with respect to band positions and intensity ratios as influenced by counterion and solvent. The neutral analogues $(\eta^5\text{-}C_5H_5)$- and $(\eta^5\text{-}C_5Me_5)Fe(CN)(CO)_2$ as well as the protonated $H[(\eta^5\text{-}C_5H_5)Fe(CN)_2(CO)]$ are included for comparison. The X-ray crystal structure of the latter finds short interionic N····N distances of 2.55 Å indicative of CN-nitrogen protonation and strong H-bonding as similarly seen in the attachment of $Fe(CN)_2(CO)$ to the protein found in the crystal structure of $[NiFe]H_2$-ase enzyme isolated from the *D. gigas* bacteria. For a series of nine complexes that covers a broad range of electronic effects (as confirmed by electrochemical studies) within a constant hexacoordinate structure and medium (CH_3CN), there is an excellent linearity in the correlation between ν(CO) (or F_{CO}) and ν(CN) (or F_{CN}). The enzyme states that are not in the catalytic cycle reasonably fit the model complex correlation and are expected to maintain hexacoordination about iron. The possibile source(s) of deviations from this correlation both in the model (in aqueous media) and in the enzyme system are discussed.

Introduction

The impressive discoveries of the organometallic fragment, $Fe(CN)_2(CO)$, cysteine-bridged to the nickel ion in *Desulfovibrio gigas* (Figure 1)[1,2] and in *Chromatium vinosum*[3] [NiFe]-hydrogenases, offer an opportunity to explore the various known enzymatic states by vibrational spectroscopy. Isolated from other vibrational modes, the triply bonded diatomic region of the IR spectrum is a powerful diagnostic tool for defining both structure and electronic effects in small-molecule transition metal complex chemistry. In fact, infrared spectra have been measured on both $[NiFe]H_2$ase enzymes,[3,4] redox poised to match states previously (prior to discovery of the heterobimetallic nature of the active site) probed by EPR spectroscopy.[5] That the EPR signals were nickel-based was confirmed by isotopic substitution of ^{61}Ni and attributed to the presence of d^7 Ni^{III} and d^9 Ni^{I} in the oxidized (inactive enzymatically) and reduced (active enzyme) forms, respectively.[5,6] Other enzymatically active forms are EPR silent and presumed to be d^8 Ni^{II} and a sub-reduced Ni^0 (or a $Ni^{II}-H$) form. The influence of the pendant $Fe(CN)_2$-

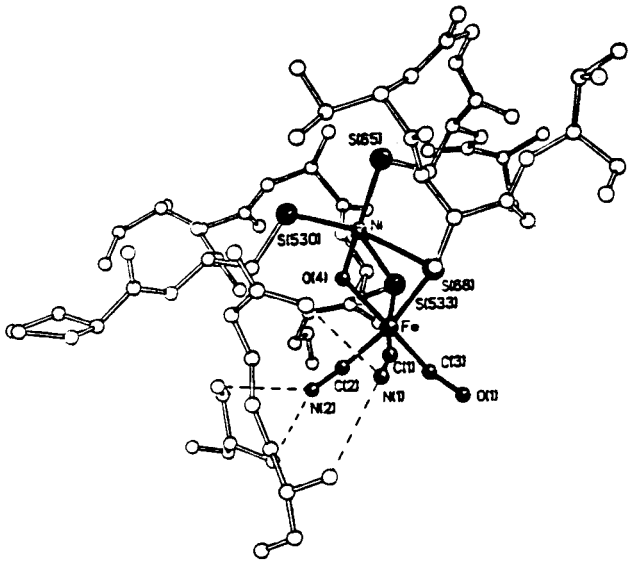

Figure 1. NiFe bimetallic site of [NiFe]hydrogenase isolated from *D. gigas*.[1,2] Produced from coordinates provided by M. Frey (personal communication).

(1) (a) Frey, M. *Struct. Bonding* **1998**, *90*, 97 and references therein. (b) Fontecilla-Camps, J. C. *J. Biol. Inorg. Chem.* **1996**, *1*, 91 and references therein.

(2) (a) Volbeda, A.; Garcin, E.; Piras, C.; de Lacey, A. L.; Fernandez, V. M.; Hatchikian, E. C.; Frey, M.; Fontecilla-Camps, J. C. *J. Am. Chem. Soc*. **1996**, *118*, 12989. (b) Volbeda, A.; Charon, M.-H.; Piras, C.; Hatchikian, E. C.; Frey, M.; Fontecilla-Camps, J. C. *Nature* **1995**, *373*, 580.

(3) (a) Happe, R. P.; Roseboom, W.; Pierik, A. J.; Albracht, S. P. J.; Bagley, K. A. *Nature* **1997**, *385*, 126. (b) Bagley, K. A.; Duin, E. C.; Roseboom, W.; Albracht, S. P. J.; Woodruff, W. H. *Biochemistry* **1995**, *34*, 5527.

(4) de Lacey, A. L.; Hatchikian, E. C.; Volbeda, A.; Frey, M.; Fontecilla-Camps, J. C.; Fernandez, V. M. *J. Am. Chem. Soc*. **1997**, *119*, 7181.

(5) Roberts, L. M.; Lindahl, P. A. *J. Am. Chem. Soc*. **1995**, *117*, 2565.

(6) (a) Lancaster, J. R. *Science* **1982**, *216*, 1324. (b) Moura, J. J. G.; Moura, I.; Huyhn, B. H.; Krüger, H. J.; Teixeira, M.; DuVarney, R. C.; DerVartanian, D. V.; Xavier, A. V.; Peck, H. D., Jr.; LeGall, J. *Biochem. Biophys. Res. Commun.* **1982**, *108*, 1388. (c) Albracht, S. P. J.; Graf, E.-G.; Thauer, R. K. *FEBS Lett.* **1982**, *140*, 311.

S0002-7863(98)02053-8 CCC: $15.00
Published on Web 09/19/1998

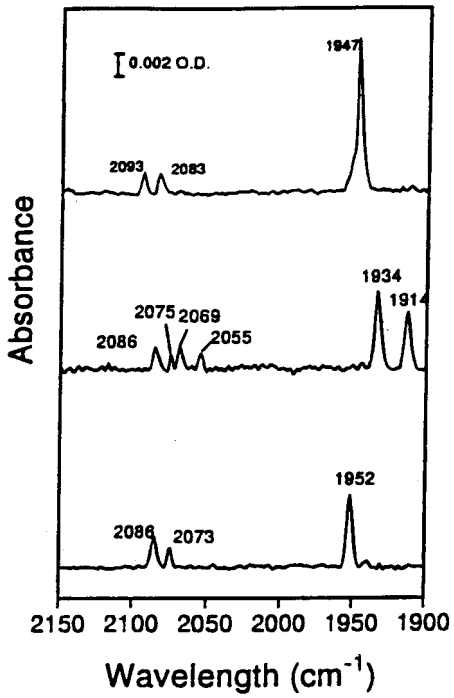

Figure 2. Selected IR spectra measured on redox poised *D. gigas* enzyme: (top) the "as isolated" or oxidized ("Ni-A") form; (middle) mixture of two of the reduced EPR silent forms; (bottom) the "Ni-C", EPR-active form. Modified from ref 4. Copyright 1997 American Chemical Society.

(CO) fragment on the nickel center, its redox activity, and its possible role in catalysis is a prime issue at this point.

Reproduced in Figure 2 are selected IR spectra in the triply bonded diatomic region of several forms of the *D. gigas* enzyme, the "as isolated" or oxidized ("Ni-A"), the one-electron-reduced ("Ni-Si") forms (there are two of these), and the enzymatically active, or two-electron-reduced, "Ni-C" form.[4] Isotopic substitutions of ^{13}CN, C^{15}N, and ^{13}CO in *C. vinosum* have assigned similar spectra for the Ni-A form;[3] the less intense bands near 2100 cm^{-1} belong to the two CN$^-$ and that at ca. 1950 cm^{-1} to CO. Detailed redox titrations correlate with other enzyme states, producing the greatest IR band shifts, as referenced to the oxidized form, for one of the states that is EPR silent and assumed to be Ni^{II}, i.e., ν(CO) = 1914 and ν(CN) = 2055 and 2069 cm^{-1}.[4] Interestingly, as the enzyme is further reduced (by one-electron, coupled with addition of a proton), the IR bands shift positively, with the result that the bands in the Ni-C form are nearly identical to that of Ni-A.

While the IR spectra of the enzyme show sensitivity to redox level, the shifts are substantially less than what has been established for mononuclear homoleptic metal carbonyls or metal cyanide complexes as the metal oxidation state is changed, or in isoelectronic series that produce a full charge change on octahedral complexes as the result of change of metal; for CO, $\Delta(\nu(\mathrm{CO}))$ = ca. 100−120 cm^{-1}, and for CN, $\Delta(\nu(\mathrm{CN}))$ = ca. 60 cm^{-1}.[7] Since there has been no spectroscopic indication of unpaired electron density on iron,[8] and X-ray absorption spectroscopic studies on redox poised enzyme find only minor changes in Ni K-edge regardless of enzyme state,[9] major changes in vibrational spectroscopy are likewise not to be expected. Clearly all aspects of the enzyme-bound heterobimetallic complex, surrounded by good H-bonding or proton-donating sites must be used to explain the effect of the redox events on spectroscopy. That is, the features that might be required in the active site (Figure 3) are intertwined and complicated beyond any available model complex. Yet, the sensitivity of vibrational spectroscopy, of fundamental importance to establishing reaction pathways and rationales of structure and bonding in organometallic chemistry, should, if carefully referenced, likewise provide definitive information in this bioorganometallic system.

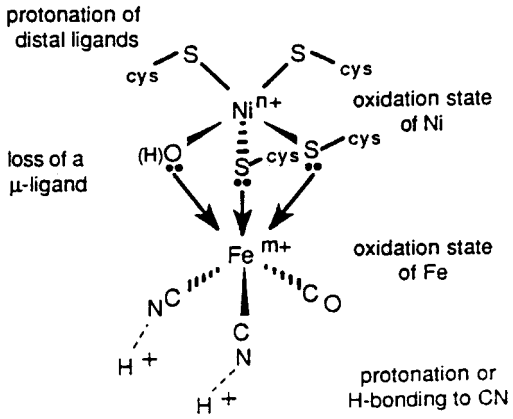

Figure 3. Features required for ideal model complex for bimetallic site of [NiFe}H_2ase. Left out are H-bondings to N.

There are few vibrational studies of complexes containing mixed CN$^-$/CO ligands with which to compare the combinational response of such ligands to electron density changes. Thus a search for a small molecule containing the pyramidal Fe(CN)$_2$(CO) unit led to the simple organometallic anion, (η^5-C$_5$H$_5$)Fe(CN)$_2$(CO)$^-$.[10] The X-ray crystal structure of the piano stool complex overlays well with the Fe(CN)$_2$(CO) moiety of the *D. gigas* enzyme, the η^5-C$_5$H$_5$ ring serving as the 6-electron donor analogue of the Ni-(μ-SCys)$_2$(μ-OH) trigonal face of the octahedral iron unit in the oxidized enzyme (Figure 4).[11] Furthermore, the organometallic is also an almost exact infrared spectral analogue for the Fe(CN)$_2$(CO) unit of the heterobimetallic active site of [NiFe]H_2ase enzyme as isolated (i.e., oxidized form) from *C. vinosum* and *D. gigas*! This fortunate, yet surprising, observation led to questions of the sensitivity of the Fe(CN)$_2$(CO) unit to electronic differences; such a close analogy of Cp$^-$ and sulfur/oxygen donor sets was not predictable a priori. In the work described below, a series of nine derivatives of the Fe diatomic unit will be used to correlate the relative responses of the CN and CO ligands to electron density changes both internally (change of facial donor ligand and Fe oxidation state) and externally (change of H-bonding and solvent interactions). Such correlation is the basis for development of diatomic IR spectroscopy as diagnostic of structure in enzyme active sites and could, as well, help formulate a rationale for the design of this extraordinary heterobimetallic catalyst.

(7) Braterman, P. S. In *Metal Carbonyl Spectra*; Academic Press: New York, 1975; Chapter 7, p 181, Table 7.3. Adams, D. M. In *Metal−Ligand and Related Vibrations: A Critical Survey of the Infrared and Raman Spectra of Metallic and Organometallic Compounds*; St. Martin's Press: New York, 1968; Chapter 3.

(8) Huyett, J. E.; Carepo, M.; Pamplona, A.; Franco, R.; Moura, I.; Moura, J. J. G.; Hoffman, B. M. *J. Am. Chem. Soc.* **1997**, *119*, 9291 and references therein.

(9) (a) Gu, Z.; Dong, J.; Allan, C. B.; Choudhury, S. B.; Franco, R.; Moura, J. J. G.; Moura, I.; LeGall, J.; Przybyla, A. E.; Roseboom, W. R.; Albracht, S. P. J.; Axley, M. J.; Scott, R. A.; Maroney, M. J. *J. Am. Chem. Soc.* **1996**, *118*, 11155. (b) Bagyinka, C.; Whitehead, J. P.; Maroney, M. J. *J. Am. Chem. Soc.* **1993**, *115*, 3576.

(10) (a) Coffey, C. E. *Inorg. Nucl. Chem.* **1963**, *25*, 179. (b) Dineen, J. A.; Pauson, P. L. *J. Organomet. Chem.* **1974**, *71*, 77.

(11) Darensbourg, D. J.; Reibenspies, J. H.; Lai, C.-H.; Lee, W.-Z.; Darensbourg, M. Y. *J. Am. Chem. Soc.* **1997**, *119*, 7903.

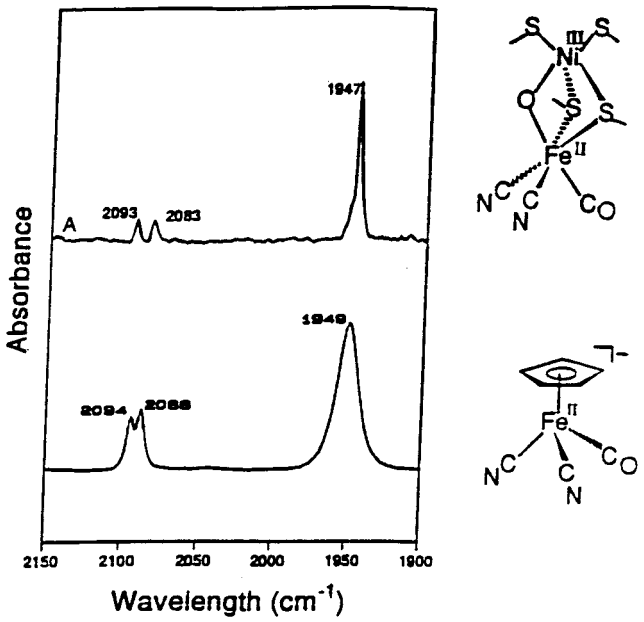

Figure 4. Comparison of IR spectra in triply bonded diatomic region for the oxidized ("Ni-A") form of *D. gigas* enzyme[4] and K[(η^5-C_5H_5)Fe(CN)$_2$(CO)] in CH_3CN solution.

Experimental Section

General Methods and Materials. All syntheses and product isolations were carried out under argon using standard Schlenk and glovebox techniques. Acetonitrile was distilled once from CaH_2 and once from P_2O_5 and freshly distilled from CaH_2 before use. Commercially available methanol was distilled from Mg turnings and iodine.

The following materials were of reagent grade and were used as purchased: cyclopentadienyliron dicarbonyl dimer and trimethyloxonium tetrafluoroborate (Aldrich Chemical Co.), (pentamethylcyclopentadienyl)iron dicarbonyl dimer (Strem Chemical Co.); ^{13}C- and ^{15}N-labeled potassium cyanide, as well as ^{13}CO and deuterated solvents (Cambridge Isotope Laboratories). Other reagents were from standard vendors and used as received.

Elemental analyses were carried out by Canadian Microanalytical Service, Ltd., Canada.

Physical Measurements. Infrared spectra were measured on a Mattson Galaxy 6021 instrument using a 0.1-mm CaF_2-sealed cell for solutions and KBr pellets for solid samples. A BAS-100A electroanalyzer utilizing a glassy carbon working electrode, Ag/$AgNO_3$ reference electrode, and platinum auxiliary electrode was used for electrochemical measurements. Cyclic voltammograms were obtained from 2.5 mM analyte concentration in CH_3CN or MeOH using 0.1 M [*n*-Bu_4N][PF_6] supporting electrolyte or in H_2O using 0.1 M KCl supporting electrolyte. All potentials were scaled to NHE using ferrocene ($E_{1/2}^{NHE} = 400$ mV in acetonitrile) or methylviologen ($E_{1/2}^{NHE} = -446$ mV in aqueous solvent) as internal standards.[12] The measurements were carried out under an Ar atmosphere and at room temperature (22 °C). EPR spectra were recorded on a Bruker ESP 300 spectrometer equipped with an Oxford ER910A cryostat at 10 K. Nuclear magnetic resonance spectra were recorded on a Varian XL-200 FT NMR spectrometer. Electrospray ionization (ESI) mass spectra were acquired using a Vestec 201A quadrupole mass spectrometer equipped with a a Technivent Vector One data system interfaced with an IBM-compatible Pentium personal computer.

Photolysis reactions were carried out in a 50-mL Schlenk flask containing a stirred methanol solution of the complex which was placed 15 cm away from a mercury arc 450-W UV lamp. The lamp was suspended in a borosilicate immersion well in which water was circulated to prevent the lamp from warming the solution during irradiation. For safety purposes, the photolysis setup was in a hood whose glass front was covered with aluminum foil.

Syntheses. Only small modifications of published procedures[10] were used to obtain the cyclopentadienyl compounds listed in Chart 1. The pentamethylcyclopentadienyl compounds are reported for the first time below or in a separate paper.[13]

Chart 1. Model Complexes

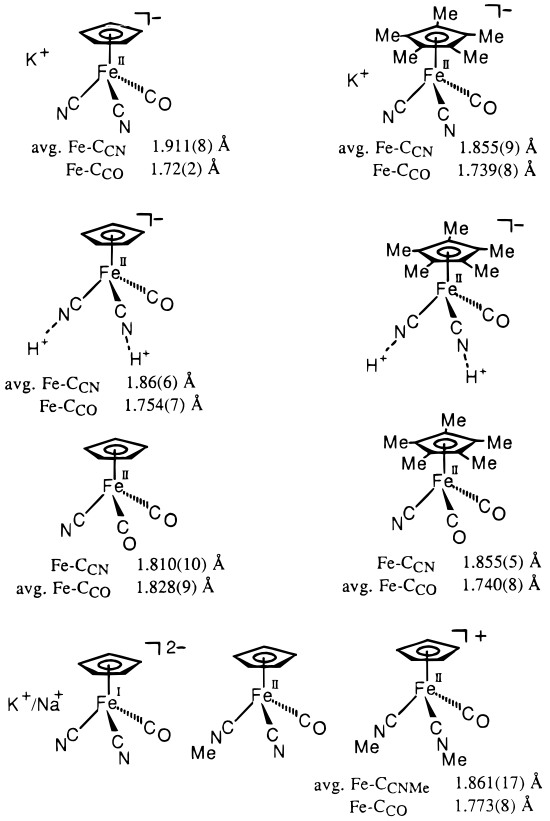

Preparation of K$^+$ and Na$^+$ Salts of [CpFe(CO)(CN)$_2$]$^-$ (Cp = η^5-C_5H_5) and H[CpFe(CO)(CN)$_2$]. The [CpFe(CO)(CN)$_2$]$^-$ salts were synthesized and isolated typically on a 0.1 scale of the published procedure.[10] Iodine as well as bromine were employed for the oxidative cleavage of [CpFe(CO)$_2$]$_2$ in MeOH; addition of aqueous solutions of KCN or NaCN followed by a short (20 min) reflux produced the desired salts as hygroscopic orange powders. Recrystallization from saturated ethanol solution gave yellow-brown crystals which were soluble in water, alcohol, and acetonitrile but insoluble in nonpolar solvents. K[CpFe(CO)(CN)$_2$]: IR: see Table 1. NMR (CD_3OD): ^{1}H 4.92 (s, 5H); ^{13}C 220.00, 154.00, 83.2. Na[CpFe(CO)(CN)$_2$]: IR: Table 1. Anal. Calcd for $C_8H_5ON_2FeNa$: C, 42.9; H, 2.3; N, 12.5. Found: C, 41.0; H, 2.4; N, 12.0.

According to Coffey's procedure,[10] an aqueous solution of K[CpFe(CO)(CN)$_2$] (1.20 g, 5 mmol, in 10 mL of water) was treated with excess concentrated HCl to precipitate a yellow powder, H[CpFe(CO)(CN)$_2$]. Upon removal of the H_2O by cannula and washing the remaining solid with ether, the crude product was obtained in 75% yield. The yellow solid is soluble in alcohols and acetone, sparingly soluble in acetonitrile, tetrahydrofuran, dichloromethane, and water, and insoluble in nonpolar solvents. X-ray quality crystals were obtained by ether diffusion into an EtOH solution. IR data: Table 1. NMR (CD_3OD, ppm): ^{1}H 5.03, 4.97; ^{13}C 217.53, 84.44, 82.68. Mass spectroscopy: (+)ESI; *m*/*z* (% intensity): 203(100), 175(61), 148(28).

Preparation of [Et$_3$NH][CpFe(CO)(CN)$_2$]. [Et_3NH][CpFe(CO)(CN)$_2$] was synthesized and isolated according to the published procedure,[10a] as follows: Addition of excess triethylamine to a 10-mL ethanolic solution of H[CpFe(CO)(CN)$_2$] (0.0808 g, 0.4 mmol) produced a dark brown solution. Further addition of a large amount of diethyl ether to the concentrated solution precipitated an air-sensitive yellow powder. The complex was soluble in water, alcohol, and acetonitrile but insoluble in nonpolar organic solvents. IR: see Table 1.

(12) (a) Gagne, R. R.; Koval, C. A.; Lisensky, G. C. *Inorg. Chem.* **1980**, *19*, 2854. (b) Bird, C. L.; Kuhn, A. T. *Chem. Soc. Rev.* **1981**, *10*, 49.

(13) Darensbourg, D. J.; Lee, W.-Z.; Reibenspies, J. H. Manuscript in preparation.

Table 1. Infrared Spectroscopic Data in ν(CO) and ν(CN) Regions

compd	condition	ν(CO), cm^{-1}	ν(CN), cm^{-1}	ν(CNR), cm^{-1}
		The Fe^{II} Species		
K[CpFe(CO)(CN)$_2$]	CH_3CN	1949	2088, 2094	
	KBr	1954, 1973	2085, 2095	
	H_2O	1979	2068, 2083	
K[CpFe(CO)(CN)(^{13}CN)]	CH_3CN	1949	2045, 2092	
K[CpFe(CO)(^{13}CN)$_2$]	CH_3CN	1951	2044, 2050	
K[CpFe(CO)(C^{15}N)$_2$]	CH_3CN	1951	2059, 2065	
K[CpFe(^{13}CO)(CN)$_2$]	CH_3CN	1907	2088, 2094	
K[CpFe(^{13}CO)(^{13}CN)$_2$]	CH_3CN	1905	2043, 2048	
Na[CpFe(CO)(CN)$_2$]	CH_3CN	1953	2093, 2103	
[Et$_3$NH][CpFe(CO)(CN)$_2$]	CH_3CN	1957	2088, 2096	
H[CpFe(CO)(CN)$_2$]	KBr	1991	2106, 2135	
	CH_3CN	1988	2096, 2107	
	$(CH_3)_2CHOH$	1975, 1996	2083, 2102, 2122	
	EtOH	1975, 1994	2088, 2099, 2118	
	H_2O	1979	2068, 2083	
CpFe(CO)(CNMe)(CN)	CH_3CN	1988	2105	2200
[CpFe(CO)(CNMe)$_2$][BF$_4$]	CH_3CN	2021		2211, 2231
CpFe(CO)$_2$(CN)	CH_3CN	2014, 2059	2121	
	THF	2003, 2051	2124	
		The Cp* Species		
K[Cp*Fe(CO)(CN)$_2$]	CH_3CN	1924	2079, 2085	
	MeOH	1948	2072, 2081	
Cp*Fe(CO)$_2$(CN)	CH_3CN	1983, 2032	2112	
		The Fe^{I} Species		
[Na][K][CpFe(CO)(CN)$_2$]	CH_3CN	1863 (sh), 1898	2063, 2071	
[Na][K][CpFe(CO)(^{13}CN)$_2$]	CH_3CN	1896	2017	
		C. vinosum[3a]		
natural abundance		1945	2083, 2093	
^{15}N-labeled		1944	2050, 2062	
^{13}C-labeled		1900	2036, 2047	

Preparation of CpFe(CO)(CNMe)(CN).[10b] A solution of K[CpFe(CO)(CN)$_2$] (0.048 g, 0.2 mmol) in 15 mL of acetonitrile was treated dropwise with a solution of [Me$_3$O][BF$_4$] (0.045 g, 0.3 mmol) in 15 mL of acetonitrile. The resulting mixture was stirred for 2 h, and the orange supernatant was transferred into another flask. An orange solid was obtained upon solvent removal in vacuo. IR: Table 1.

Preparation of [CpFe(CO)(CNMe)$_2$][BF$_4$]. As described previously,[10b] a mixture of K[CpFe(CO)(CN)$_2$] (0.048 g, 0.2 mmol) and [Me$_3$O][BF$_4$] (0.090 g, 0.6 mmol) in 30 mL of acetonitrile was stirred for 2 h. A yellow-orange solution was transferred to another flask via cannula. Upon removal of solvent, an orange complex was obtained in ca. 75% yield.

Preparation of Cp*Fe(CO)$_2$(CN) (Cp* = η^5-C$_5$Me$_5$) and K[Cp*Fe(CO)(CN)$_2$]. According to the procedure published for the isolation of CpFe(CO)$_2$(CN),[10a] addition of Br$_2$ to [Cp*Fe(CO)$_2$]$_2$ in methanol was followed by stirring for 2 h at 22° to produce Cp*Fe(CO)$_2$Br. In the same flask 1 equiv of KCN was added, followed by heating at 50 °C for 2 h. The resulting solution was evaporated to yield an orange powder in 43% yield. Cp*Fe(CO)$_2$(CN): IR: Table 1. Anal. Calcd for C$_{13}$H$_{15}$O$_2$NFe: C, 57.2; H, 5.5; N, 5.1. Found: C, 57.0; H, 5.5; N, 5.0. CpFe(CO)$_2$(CN): IR: see Table 1. Anal. Calcd for C$_8$H$_5$O$_2$NFe: C, 47.3; H, 2.5; N, 6.9. Found: C, 47.2; H, 2.4; N, 6.9.

Whereas the CpFe(CO)(CN)$_2^-$ anion is prepared by thermal substitution of CO in CpFe(CO)$_2$(CN) by CN$^-$, the Cp* analogue requires photolysis. A mixture of Cp*Fe(CO)$_2$(CN) (0.055 g, 0.2 mmol) and KCN (0.015 g, 0.23 mmol) was loaded into a 50-mL standard Schlenk flask, and dissolved with 30 mL of methanol. UV photolysis, described above, was applied for 4 h. The orange solid that was obtained upon evaporation of solvent from the resulting solution was extracted with 30 mL of degassed acetonitrile. Subsequent solvent removal produced an orange solid which was washed with diethyl ether and dried in vacuo, in 78% yield. IR: Table 1. X-ray quality crystals, containing an ether molecule in the crystal lattice, were obtained by ether diffusion into an acetonitrile solution.

Preparation of [Na][K][CpFe(CO)(CN)$_2$] and K$_2$[CpFe(CO)(CN)$_2$]. Yellow K[CpFe(CO)(CN)$_2$] (0.24 g, 1 mmol in 30 mL CH_3CN) was added to a Na/Hg amalgam (15 mL) containing 0.15 g of sodium metal; the mixture was stirred for 1 h. The resulting yellow solution was filtered through anhydrous Celite on a Schlenk filter. Upon removal of solvent from the filtrate and washing with diethyl ether, a yellow semisolid was obtained in ca. 30% yield, assuming the above formulation. IR: Table 1. EPR: $g = 4.25, 1.99$. Extreme air and moisture sensitivity prevented elemental analysis. Mass spectroscopy: (−)ESI *m*/*z* 215(17), 201(87), 187(26), 173(100). Similar spectral results were obtained on the salt isolated using a K/Hg amalgam.

Preparation of Isotopically Labeled Compounds. The isotopically labeled [CpFe(CO)(CN)$_2$]$^-$ salts enriched to greater than 98% in ^{13}CN or C^{15}N were prepared according to Coffey's syntheses,[10] substituting the correspondingly isotopically labeled KCN salts, typically on a microgram scale. Photolysis of an ethanol solution of [K][CpFe(CO)(CN)$_2$] in the presence of ^{13}CO for 3 h results in [K][CpFe(^{13}CO)(CN)$_2$] enriched to greater than 90% in ^{13}CO.

High dilution optimized the yield of the mixed isotopic dicyanide complex K[CpFe(CO)(CN)(^{13}CN)]. A mixture of CpFe(CO)$_2$(CN) (10 mg, 0.05 mmol) and K(^{13}CN) (3.3 mg, 0.05 mmol) dissolved in in 30 mL of methanol was refluxed for 20 h. The resulting yellow solution was evaporated to dryness, and the product was extracted with 20 mL of acetonitrile to provide a small amount of K[CpFe(CO)(CN)(^{13}CN)]. IR: see Table 1.

X-ray Crystal Structures. The X-ray crystal structures were solved at the Crystal & Molecular Structure Laboratory Center for Chemical Characterization and Analysis at Texas A&M University. X-ray crystallographic data were obtained on a Siemens R3m/V single-crystal X-ray diffractometer operating at 55 kV and 30 mA, M*o* Kα (λ = 0.710 73 Å) radiation equipped with a Siemens LT-2 cryostat. Diffractometer control software P3VAX 3.42 was supplied by Siemens Analytical Instruments, Inc. All crystallographic calculations were performed with use of the Siemens SHELXTL-PLUS program package.[14] The structures were solved by direct methods. Anisotropic refinement for all non-hydrogen atoms was done by a full-matrix least-squares method. A single crystal was mounted on a glass fiber with epoxy cement at 193 K in an N$_2$ cold steam. Cell parameter and data

Table 2. X-ray Crystallographic Data for H[(η^5-C_5H_5)Fe(CO)(CN)$_2$] and K[(η^5-C_5Me_5)Fe(CO)(CN)$_2$]

	H[(η^5-C_5H_5)-Fe(CO)(CN)$_2$]	K[(η^5-C_5Me_5)-Fe(CO)(CN)$_2$]
chemical formula	$C_8H_5FeN_2O$	$C_{15}H_{20}FeKN_2O_{1.50}$
formula wt (g/mol)	201.0	347.28
temperature, K	193(2)	193(2)
wavelength, Å	0.71073	0.71073
crystal system	orthorhombic	monoclinic
space group	*P*2(1)2(1)2(1)	*P*2(1)/*n*
unit cell dimensions	a = 6.4864(8) Å; α = 90°	a = 8.710(4) Å; α = 90°
	b = 11.0920(12) Å; β = 90°	b = 14.360(4) Å; β = 95.01(5)°
	c = 11.8935(14) Å; γ = 90°	c = 28.160(2) Å; γ = 90°
volume, Å^3	855.70(17)	3509(3)
Z	4	8
ρ calculated, Mg/m^3	1.560	1.315
absorption coeff, mm^{-1}	1.709	1.097
$S(F^2)$[a]	1.043	1.097
absorption correction	PSI-scans	PSI-scans
$R(F)$ [$I > 2\sigma(I)$],[a]%	4.03	7.36
$_wR(F^2)$ all data,[a] %	9.13	20.88

[a] Residuals: $R(F) = \sum|F_o - F_c|/\sum F_o$; $_wR(F^2) = \{\sum w(|F_o^2| - |F_c^2|)^2/[\sum w(F_o^2)^2]\}^{1/2}$.

collection summaries for compounds K[Cp*Fe(CO)(CN)$_2$] and H[CpFe(CO)(CN)$_2$] are given in Table 2.

Results and Discussion

The Model Complexes. Chart 1 contains stick drawings of the nine complexes included in this study. While the η^5-C_5H_5 (Cp) derivatives have been known for many years, the η^5-C_5Me_5 (Cp*) compounds are first reported here. Six of the complexes have been characterized by X-ray crystallography. That of the K[CpFe(CN)$_2$(CO)] salt was presented earlier;[11] its acid form, H[CpFe(CN)$_2$(CO)], is first reported below, as is the K[Cp*Fe(CN)$_2$(CO)] salt as its ether solvate. Details of the structures of the neutral CpFe(CO)$_2$CN and Cp*Fe(CO)$_2$CN as well as the dimethylated or bis(methylisonitrile) cation, CpFe(CO)(CNMe)$_2^+$, will be reported separately.[13] The dianionic iron(I) derivative was prepared by Na/Hg amalgam reduction of K[CpFe(CN)$_2$(CO)] and characterized by IR shifts (see below) of the ν(CO) and ν(CN) to lower wavenumbers as expected, shifts with ^{13}CN isotopic labeling, as well as an EPR signal at g = 1.993 consistent with a $S = {}^1/_2$ spin state, i.e., low-spin d.[7] A signal at g = 4.23, ubiquitous in iron samples and assumed to be an impurity, is also seen.[15] Attempts to further characterize the Fe^{I} species by oxidation (using outer-sphere oxidants Ce^{IV} and Cp$_2$Fe$^+$) led to complicated mixtures. The most successful reclaimation of the Fe^{II} species was via protonation which yielded (presumably) H_2 and a product spectroscopically similar to H[CpFe(CN)$_2$(CO)].

X-ray Crystal Structures. Figure 5 presents the crystal packing diagram of protonated [CpFe(CN)$_2$(CO)], and Figure 6 shows the thermal ellipsoid drawing of a single molecule. The extended structure of H[CpFe(CN)$_2$(CO)] finds all cyanides in alignment with a cyanide from an adjacent molecular anion with N···N distances of 2.55 Å as is typical of strong H-bonding.[16] This observation, coupled with the substantial similarity in the angular data of the coordination spheres of iron in the K[CpFe(CN)$_2$(CO)] and the H[CpFe(CN)$_2$(CO)] forms, confirms protonation is at the cyanide nitrogen, and the formula might be expressed as CpFe(CNH)(CN)(CO).[16] However, both cyanides are interacting equally well with protons, and there is no NMR evidence for a distinct CNH ligand in solution. Therefore we will retain the formulation of H[CpFe(CN)$_2$(CO)] which at minimum expresses the fact of outer-sphere protonation. The strong network of H-bonding throughout the crystal lattice accounts for the low solubility of the acid form in aprotic solvents. Strong nucleophilicity of cyanide nitrogen is also seen in reactions of the [CpFe(CN)$_2$(CO)]$^-$ anion with methyl iodide and BF_3 which readily yield methylisonitrile derivatives and N-bound adducts of BF_3.

As was found for the K[CpFe(CN)$_2$(CO)] salt, the structure of K[Cp*Fe(CN)$_2$(CO)]·(C_2H_5)$_2$O (Figure 7) shows extensive contact ion pairing interactions of K$^+$ and cyanide. The permethylated Cp ring as well as the inclusion of a (C_2H_5)$_2$O solvating K$^+$ accounts for the different crystal lattices of the Cp* as compared to the Cp derivative; all other geometrical

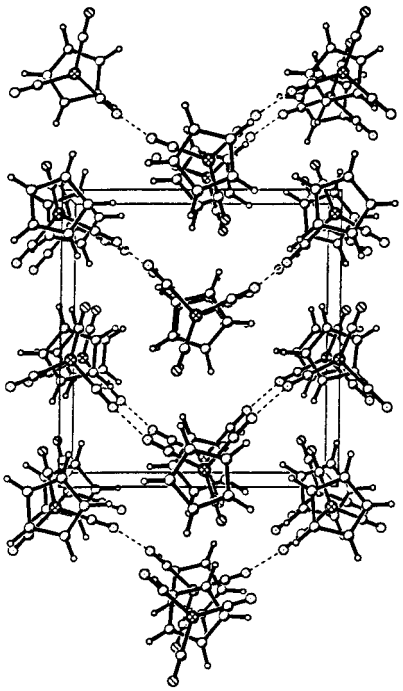

Figure 5. Crystal packing diagram for H[(η^5-C_5H_5)Fe(CN)$_2$(CO)].

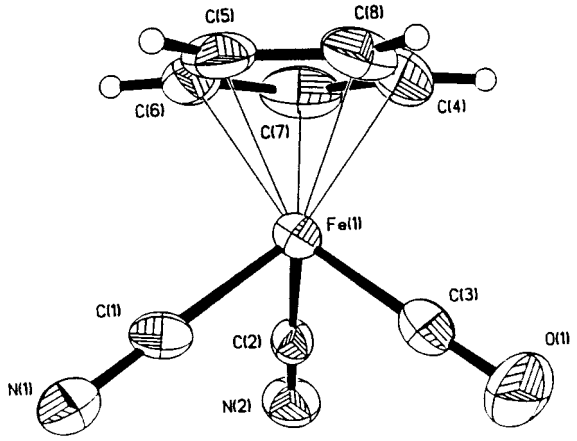

Figure 6. Thermal ellipsoid plot at 50% probability level for a molecule of H[(η^5-C_5H_5)Fe(CN)$_2$(CO)].

(14) (a) Sheldrick, G. *SHELXTL-86 Program for Crystal Structure Solution*; Institüt für Anorganische Chemie der Universität, Tammanstrasse 4, D-3400 Gottingen, Germany, 1986. (b) Sheldrick, G. *SHELXTL-93 Program for Crystal Structure Solution*; Institüt für Anorganische Chemie der Universität, Tammanstrasse 4, D-3400 Gottingen, Germany, 1993.

(15) Maeda, Y.; Kawano, K.; Oniki, T. *J. Chem. Soc., Dalton Trans.* **1995**, 3533.

(16) Fehlhammer, W. P.; Fritz, M. *Chem. Rev.* **1993**, *93*, 1243.

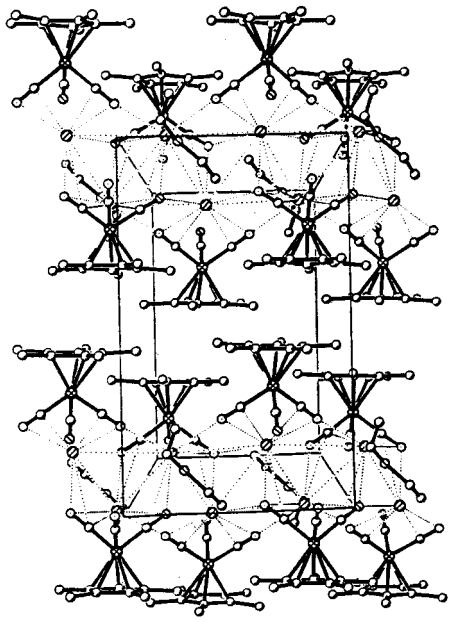

Figure 7. Crystal packing diagram for K[(η^5-C_5Me_5)Fe(CN)$_2$(CO)].

and metrical parameters are substantially the same. As in the Cp analogue, the [Cp*Fe(CN)$_2$(CO)] anion is a typical three-legged piano stool with substantially linear Fe−CN and Fe−CO groups, oriented at ca. 90° angles to each other. The average Fe−C_{Cp^*} distance is 2.11 Å, the two Fe−C_{CN} distances average to 1.855(8) Å, and the Fe−C_{CO} is 1.740(8) Å. The C−N and C−O distances are typical 1.20(1) (av) and 1.156(8) Å, respectively. The K^+ is in close contact with cyanides and the ether molecule in distorted octahedral geometry, which produces an extended structure with the CO directed into the hydrophobic region of the extended structure.

The coordination spheres of all compounds in Chart 1 are of pseudo-octahedral geometry about iron; the Fe- - -C_{Cp} and Fe- - -C_{Cp^*} average to 2.10 and 2.11 Å, respectively. The Fe−C_{CO} and Fe−C_{CN} distances are listed under the stick drawings of Chart 1.

Vibrational Spectroscopy. As illustrated in Figure 4 there is a striking similarity between the infrared spectra in the ν(CO) and ν(CN) regions of the as-isolated or oxidized form of the [NiFe]H_2ase enzyme system and K[CpFe(CO)(CN)$_2$] in acetonitrile, readily ascribed to the symmetric and asymmetric stretching vibration of the two cyanide ligands near 2100 cm^{-1} and the ν(CO) at 1949 cm^{-1} in the pyramidal [Fe(CO)(CN)$_2$] unit. Importantly, this likeness in infrared spectra carries through for all the isotopically substituted species (see Table 1 and Figure 8a,e,f). It is noteworthy that we are able to synthesize ^{13}C-labeled CO and CN derivatives independently, i.e., CpFe(^{13}CO)(CN)$_2^-$ and CpFe(CO)(^{13}CN)$_2^-$ in addition to CpFe(^{13}CO)(^{13}CN)$_2^-$, something which is not possible by the in vivo synthesis of the hydrogenase enzyme in a ^{13}C-enriched medium. In addition, we report herein the preparation and infrared spectrum of the mono-^{13}CN-labeled anion, CpFe(CO)(CN)(^{13}CN)$^-$. Unfortunately, the CO and/or CN ligands in the unlabeled enzyme have thus far not been found to undergo ligand substitution reactions with either ^{13}CN$^-$ or ^{13}CO. [A potential product of such substitution reactions is the [K]$_2$[CpFe(CN)$_3$] derivative which we have isolated and structurally characterized.][13]

The isotopic substitutions produce the expected mass difference shifts in the ν(CO) and ν(CN) vibrational modes (see the Supplementary Information). In all of the specifically isotopically labeled [Fe(CO)(CN)$_2$] species, in both the enzyme and the organometallic derivative, the ν(CO) and ν(CN) vibrational frequencies of the nonisotopically labeled ligands are essentially unaffected. This is evidence of very weak vibrational coupling between the ν(CO) and ν(CN) modes. On the other hand, there is a small difference in the interaction force constant for the two CN moieties in the two environments, with the enzyme unit displaying a slightly larger interaction force constant (k_i) of 0.079 vs 0.048 dyn/cm in the model complex.[17−19]

Although the frequencies of the respective vibrational modes are almost identical in the model and the enzyme systems, at first glance, the absolute intensity ratio of the CO versus the CN vibrations appears to be different. Indeed, what is apparent upon close examination of the two spectra in Figure 4 is that the bandwidth at half-height ($\Delta\nu_{1/2}$) for the ν(CO) bands in the two environments are quite different, i.e., 17.0 cm^{-1} (model) vs 4.0 cm^{-1} (enzyme), leading to an absolute intensity ratio almost the same in the two systems (3.7 (model) vs 3.8 (enzyme)).[20] It is well-established that $\Delta\nu_{1/2}$ values for CO stretching vibrations in metal−CO species are extremely sensitive to the solvent environment, being much more narrow in inert or noninteracting solvents.[21] *Recall* that in the enzymatic system the CO ligand resides in a hydrophobic pocket. For comparison, the $\Delta\nu_{1/2}$ value for the ν(CN) vibration in the hexane-soluble, closely related neutral organometallic derivative, Cp*Fe(CO)$_2$CN, was measured and found to be not significantly different from that in the CpFe(CO)(CN)$_2^-$ anion; however, the CO vibrational modes have $\Delta\nu_{1/2}$ values of only 4.0 cm^{-1}. On the other hand, as anticipated, the $\Delta\nu_{1/2}$ values for the ν(CO) vibrations in this derivative in the polar solvent CH_3CN are 13 cm^{-1} (see Figure 9). *Hence, the organometallic K[CpFe(CO)(CN)$_2$] derivative originally synthesized mimics all of the vibrational spectral features of the Fe(CO)(CN)$_2$ unit in the as-isolated, oxidized enzymatic system, including the diatomic stretching frequency intensity ratios.*

To examine the effect of electronic changes at the metal center on the ν(CN) and ν(CO) stretching modes, we have prepared the better electron-donating pentamethylcyclopentadienyl (Cp*) derivatives. In addition, the potassium counterion has been replaced by the proton and the methyl cation to provide the derivatives H[Fe(Cp)(CO)(CN)$_2$] and CpFe(CO)(CN)(CNMe). Further methylation of the second iron-bound CN ligand has led to the cationic species, CpFe(CO)(CNMe)$_2^+$. The resultant spectral changes are shown in Figure 10 and listed in Table 1. The positive shift in ν(CO) is the same for both protonation and methylation (both at CN^-), and there is a smaller but positive shift in ν(CN). The second methylation shifts ν(CO) positively by 33 cm^{-1}, and the methylisonitrile ν(CN) appears at >2200 cm^{-1}. Note the intensity enhancement in the CN stretch of the good π-back-bonding MeNC ligands.

The one-electron chemical reduction of K[CpFe(CO)(CN)$_2$] produced the iron(I) derivative, CpFe(CN)$_2$(CO)$^{2-}$, which as seen in Table 1 shows negative shifts in ν(CO) (−50 cm^{-1})

(17) These were calculated using a restricted force field containing only CN and CO energy-factored stretching vibrations. Furthermore, the interaction constant between CO and CN stretching motions was experimentally determined to be near zero. The $F_{CN,\,CN'}$ (90° adjacent) interaction constant in the Au(CN)$_4^-$ anion has been reported to be 0.026 mdyn/Å[18] and 0.00 in the group 12 metal tetracyanide anions.[19] This interaction constant is generally negative in sign for opposite (180°) CN, CN′ interaction constants.

(18) Jones, L. H. *Inorg. Chem.* **1965**, *4*, 1472.

(19) Jones, L. H. *Spectrochim. Acta* **1961**, *17*, 188.

(20) The ν(CO) band in the enzymatic system has two small shoulders on the high frequency side of the strong peak at 1947 cm^{-1}. These were included in the intensity measurement.

(21) (a) Adams, D. M. *Metal−Ligand and Related Vibrations*; St. Martin's Press: New York, 1968. (b) Braterman, P. S. *Metal Carbonyl Spectra*; Academic Press: New York, 1975.

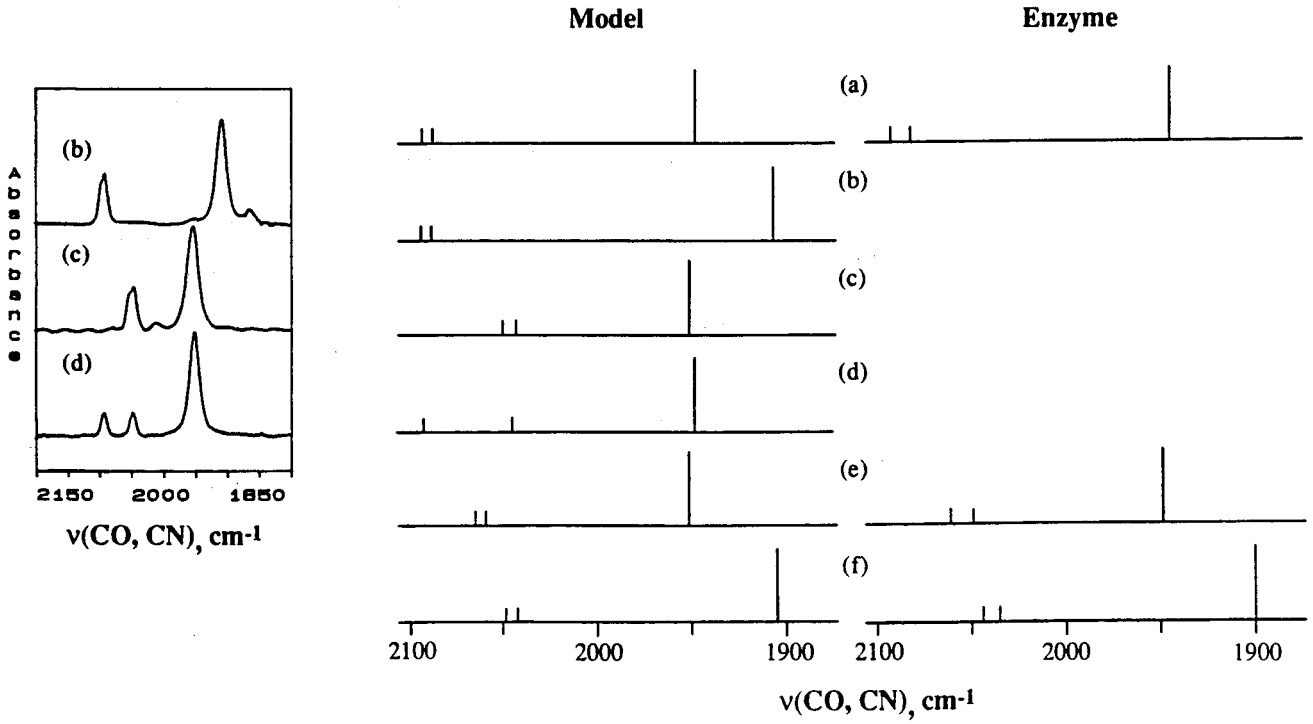

Figure 8. Line drawings of the infrared spectra in the $\nu_{CO,CN}$ region of the [Fe(CO)(CN)$_2$] unit in the *model complex*, [K][CpFe(CO)(CN)$_2$], in acetonitrile and in the *enzyme*:[3] (a) all ^{12}C, ^{14}N species; (b) ^{13}CO-labeled species; (c) di-^{13}CN labeled species; (d) mono-^{13}CN-labeled species; (e) di-C^{15}N-labeled species; (f) all ^{13}C-labeled species. The original spectra of the uniquely labeled derivatives (b, c, and d) of the model complex are given on the left.

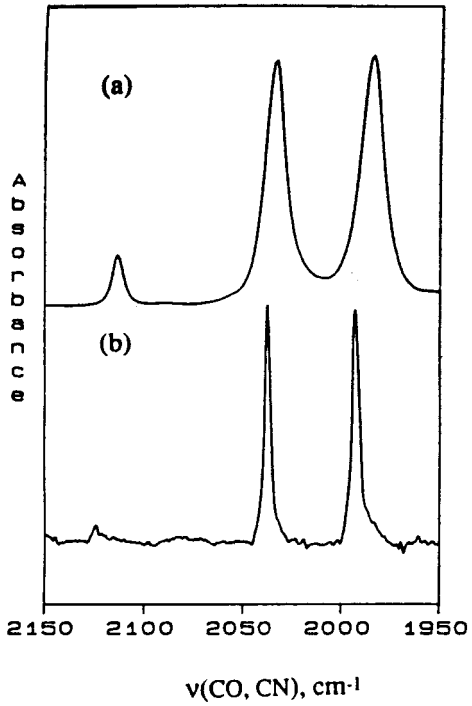

Figure 9. Infrared spectra of Cp*Fe(CO)$_2$CN in (a) CH_3CN solution and (b) hexane solution.

and ν(CN) (-24 cm^{-1}). Interestingly, the neutral dicarbonyl derivatives, CpFe(CO)$_2$CN and Cp*Fe(CO)$_2$CN, also listed in Table 1, exhibit significant CO$-$CN stretching interaction force constants with k_i' values of about 0.24 mdyn/Å.[22]

Figure 11 displays the excellent correlation exhibited between the ν(CO) and ν(CN) vibrational modes or alternatively between the corresponding stretching force constants (Table 4), F_{CO} and F_{CN}. Both plots show good linearity with a slope of 2.6, indicating that the CO vibrational mode is more greatly influenced by electronic changes at the iron center than the CN modes. Nevertheless, CN^- and CO respond to both internal and external environment changes in the same manner.

Aqueous Solution Spectra. The [K][CpFe(CN)$_2$(CO)] salt is highly soluble in water, and the aqueous solution infrared spectrum is distinct from that recorded in CH_3CN. Notably, in water, the ν(CN) modes are displaced to lower wavenumbers with a greater band separation (2083 and 2068 cm^{-1}) and the CO band is shifted to higher energy, 1979 cm^{-1}. Similar to observations in CH_3CN, the ν(CO) and ν(CN) are very weakly coupled as revealed by the infrared spectrum of the ^{13}C-labeled derivative, [K][CpFe(CO)(^{13}CN)$_2$], in water, where the ν(CO) vibration is only slightly affected by ^{13}CN substitution. The corresponding CO and CN stretching force constants computed from frequencies observed in aqueous solution were determined to be $F_{CO} = 15.81_6$, $F_{CN} = 16.39_2$ and $k_i = 0.119$ mdyn/Å. These vibrational shifts between aprotic and protic media are attributed to solvation of K^+ with water, removing it from the cation/anion interaction at cyanide, with concomitant solvation of the organometallic anion by water. Consistent with this interpretation, the infrared spectrum of the protonated derivative, [H][CpFe(CO)(CN)$_2$], in aqueous solution is identical in every respect to that of the potassium salt in water. An additional striking difference in the infrared spectra of the CpFe(CO)(CN)$_2^-$ anion in CH_3CN vs water is the relative absolute intensity ratio of the ν(CO) to ν(CN) modes. That is, this ratio is 3.7 in CH_3-CN and decreases to 1.5 in water. Presumably, the increase in the ν(CN) intensities is the result of enhanced π-accepting ability of the cyanide ligand upon interaction with the protic medium.[23]

The fact that the IR spectrum of [K][CpFe(CO)(CN)$_2$] in the aprotic solvent CH_3CN is more alike that of the oxidized enzyme strongly suggests a similar electronic environment for the Fe-(CN)$_2$(CO) moiety, which is buried within the enzyme. The

(22) Darensbourg, D. J. *Inorg. Chem.* **1972**, *11*, 1606.

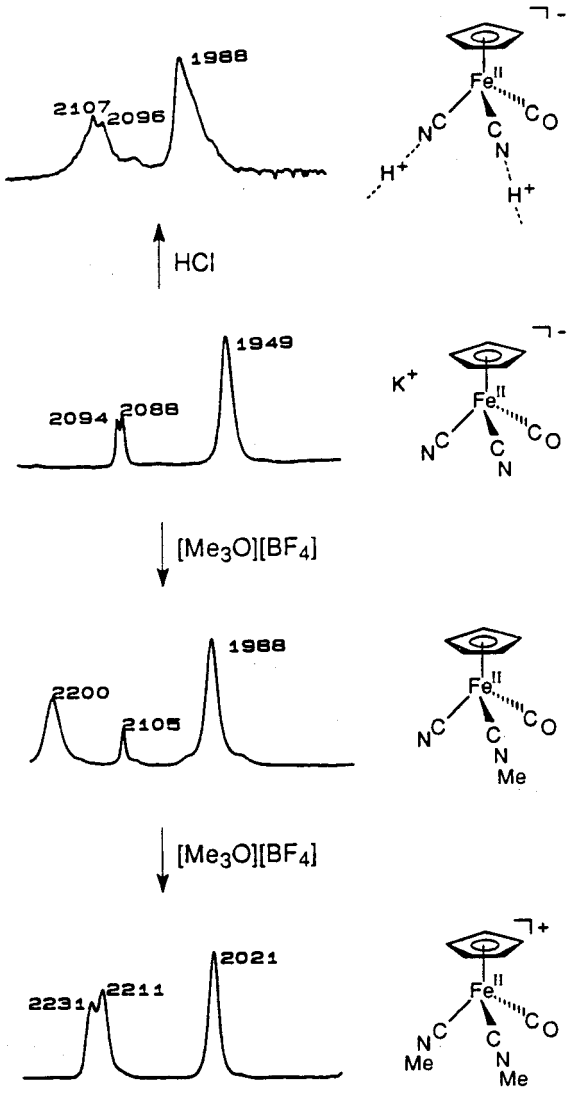

Figure 10. Infrared spectral changes (CH_3CN solution spectra) observed upon modifying the model complex, [K][CpFe(CO)$(CN)_2$], at the cyanide ligands. Bottom spectrum at reduced scale.

enzyme shows specific hydrogen-bonding interactions with the cyanides with peptide NH and OH groups, while the CO is surrounded by hydrophobic residues. *We conclude that these H-bonding interactions are more akin to the K^+ ion pair interactions to the cyanides of the model complex in aprotic media than to the optimal H-bonding interactions possible in aqueous solution.*

Electrochemistry. The cyclic voltammogram of K[CpFe(CO)$(CN)_2$] measured in CH_3CN is shown in Figure 12 and is representative of salts of CpFe(CO)$(CN)_2^-$ and Cp*Fe(CO)$(CN)_2^-$. Electrochemical data are summarized in Table 5. An irreversible cathodic peak is seen at a very negative potential (for K[CpFe(CO)$(CN)_2$], −2.33 V vs NHE) and is attributed to the electrochemical production of the 19-electron iron(I) species $[CpFe(CO)(CN)_2]^{2-}$. This highly air- and moisture-sensitive dianion was produced by bulk chemical reduction (Na/Hg amalgam) and characterized as described above. Its instability in the electrochemical cell is not easily explained as techniques to rigorously exclude both O_2 and H_2O were followed; the measurements were taken inside the Ar-filled glovebox,and it was demonstrated that the product of bulk chemical reduction

(23) As can be readily seen in Figure 10 for the CH_3NC−Fe derivative, the ν(CN) vibration is greatly enhanced in intensity relative to the NC−Fe function in the same derivative as a result of the isocyanide's increased π-acceptor property. A similar intensity enhancement would be expected for derivatives containing strong H···NC−Fe interactions. That is, in aqueous solutions it is possible to optimize this interaction compared to what is possible in the restricted hydrogen-bonding environment of the enzymatic system.

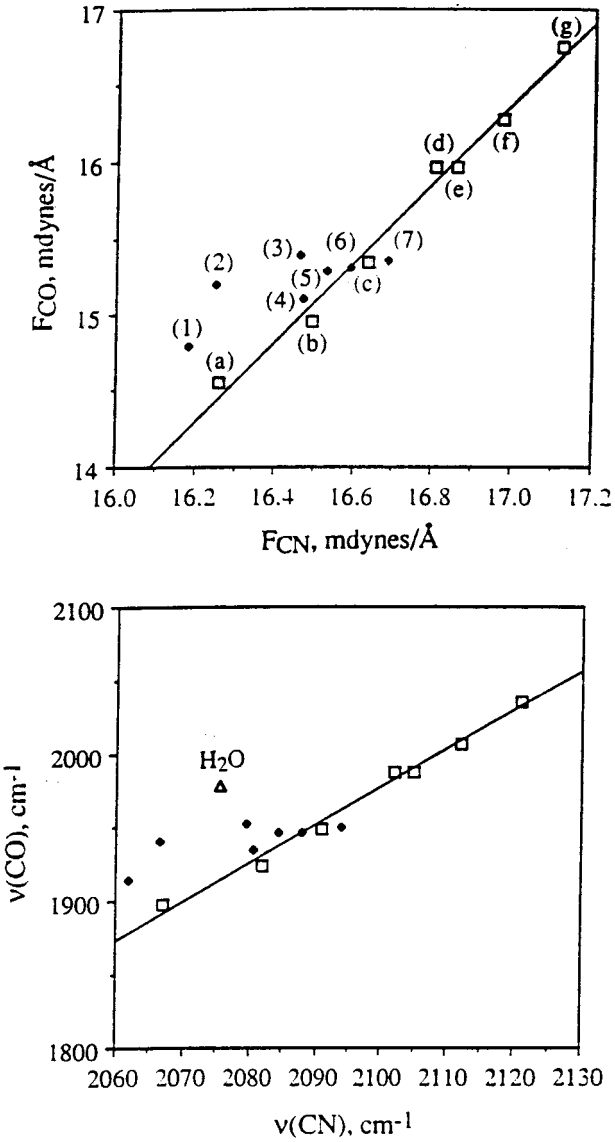

Figure 11. Correlation of ν(CO) vs ν(CN) or F_{CO} vs F_{CN} for various organometallic derivatives containing $Fe(CO)_x(CN)_y$ units (*data contained in Tables 1 and 4*). (a), (b), (c), (d), (e), (f), and (g) come from the model system as defined in Table 4. (1), (2), (3), (4), (5), (6), and (7) come from the enzyme system[4] as defined in Table 4. In the ν(CO) vs ν(CN) plot, the point labeled with H_2O is the model compound, K[(η^5-C_5H_5)Fe$(CN)_2$(CO)], in aqueous solution (*data contained in Table 1*).

Table 3. X-ray Structure Metric Data for K[CpFe(CO)$(CN)_2$], H[CpFe(CO)$(CN)_2$], and K[Cp*Fe(CO)$(CN)_2$]

	K[CpFe(CO)-$(CN)_2$][11]	H[CpFe(CO)-$(CN)_2$]	K[Cp*Fe(CO)-$(CN)_2$]
Fe−C(1)N(1) (Å)	1.918(8)	1.855(6)	1.869(9)
Fe−C(2)N(2) (Å)	1.903(8)	1.867(6)	1.841(8)
Fe−C(3)O (Å)	1.72(2)	1.754(7)	1.739(8)
C(1)−N(1) (Å)	1.143(10)	1.163(7)	1.187(11)
C(2)−N(2) (Å)	1.156(10)	1.159(7)	1.211(9)
C(3)−O(1) (Å)	1.12(2)	1.136(7)	1.156(9)
Fe−C_{cp}(av) (Å)	2.11	2.09	2.11
∠C(1)−Fe−C(2) (deg)	90.0(3)	88.0(2)	87.0(4)
∠C(1)−Fe−C(3) (deg)	94.7(7)	93.8(3)	94.4(4)
∠C(2)−Fe−C(3) (deg)	94.5(7)	92.0(3)	91.8(3)

Table 4. CO and CN Stretching Force Constants for the $Fe(CO)_x(CN)_y$ Fragment in a Variety of Organometallic Compounds and Selected Enzymatic States

compd[a,b]	F_{CO} (mdyn/Å)[c]	F_{CN} (mdyn/Å)[d]
(a) [Na][K][CpFe(CO)(CN)$_2$]	14.54_7	16.25_8 (0.062_9)
(b) K[Cp*Fe(CO)(CN)$_2$]	14.94_9	16.49_4 (0.047_5)
(c) K[CpFe(CO)(CN)$_2$]	15.34_0	16.63_8 (0.048)
(d) H[CpFe(CO)(CN)$_2$]	15.96_0	16.80_5 (0.088)
(e) CpFe(CO)(CNMe)(CN)	15.96_0	16.86_1
(f) Cp*Fe(CO)$_2$(CN)	16.27_7 (0.39_7)	16.97_3
(g) CpFe(CO)$_2$(CN)	16.75_0 (0.37_0)	17.11_8
(1) $NiSI_{1914}$	14.79_4	16.18_0 (0.110)
(2) NiR	15.19_8	16.25_0 (0.102)
(3) NiC	15.38_7	16.46_4 (0.111)
(4) $NiSI_{1934}$	15.10_5	16.47_1 (0.087_1)
(5) NiB	15.29_3	16.53_4 (0.087_3)
(6) NiA	15.30_8	16.59_0 (0.079_5)
(7) NiSU	15.35_5	16.68_5 (0.079_7)

[a] All infrared spectra for the organometallic derivatives were determined in CH_3CN. [b] Infrared spectra for enzymatic systems were measured in 100 mM Tris/KCl buffer, 100 mM KCl.[4] [c] Values in parentheses represent the CO−CO interaction force constants. [d] Values in parentheses represent the CN−CN interaction force constants.

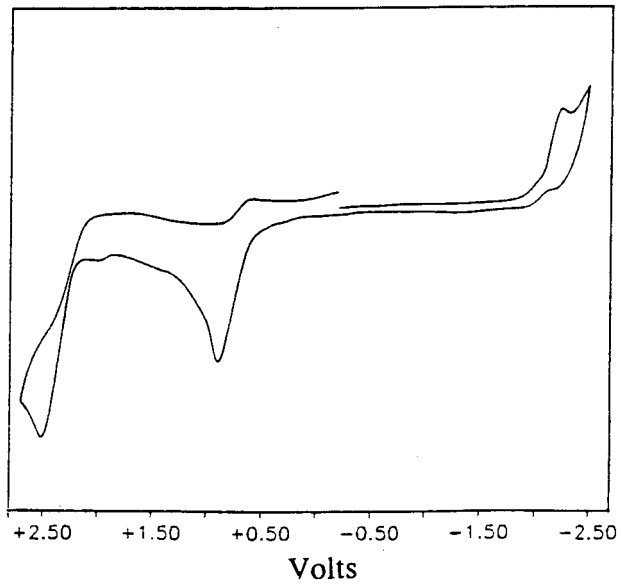

Figure 12. Cyclic voltammograms of 2.5 mM solutions of K[(η^5-C_5H_5)Fe(CN)$_2$(CO)] in 0.1 M TBAHFP/CH_3CN with a glassy carbon working electrode at a scan rate of 250 mV/s. All potentials are scaled to NHE using Cp_2Fe^+/Cp_2Fe as the internal standard ($E_{1/2}$ = 0.40 V).[12a]

is stable in the presence of the electrolyte, $Bu_4N^+BF_4^-$. It is however known that Fe(I) cyanides are labile, vide infra, perhaps in the electrochemical cell, leading to the observed deposits and degradation of the electrode surface.

As seen in Table 5, exchange of the K^+ ion by the Na^+ ion, i.e., producing Na[CpFe(CO)(CN)$_2$], stabilizes the irreversible cathodic event by +30 mV, attributed to a stronger ion-pair interaction between the sodium ion and cyanide ligands as indicated from the IR data. This Fe−CN^-···Na^+ interaction is expected to increase the π acceptor ability of the cyanide ligand and better delocalize the developing anionic charge.[24] Consistently, this reduction event is not observed for K[Cp*Fe(CO)(CN)$_2$]; the better electron donor $Me_5C_5^-$ evidently shifts the reduction beyond the solvent window (−2.5 V for CH_3CN).[25] For comparison, the $Fe^{II/I}$ potential of the cationic complex

Table 5. Listing of Electrochemical Data[a] for [CpFe(CO)(CN)$_2$]$^-$, [Cp*Fe(CO)(CN)$_2$]$^-$, CpFe(CO)$_2$(CN), and Cp*Fe(CO)$_2$(CN); Solvent and Counterion Dependencies

	E_{pc}, V[b]	$E_{1/2}(Fe^{II/III})$, V[c]	ΔE_p, mV	I_{pa}/I_{pc}
		K[CpFe(CO)(CN)$_2$]		
CH_3CN	−2.33	0.66	77	2.27
CH_3OH		0.83	60	1.29
H_2O		1.09[b]		
		Na[CpFe(CO)(CN)$_2$]		
CH_3CN	−2.30	0.71	60	1.81
CH_3OH		0.86	64	4.48
		[Et_3NH][CpFe(CO)(CN)$_2$]		
CH_3CN		0.68	59	1.62
CH_3OH		0.86	88	1.57
		H[CpFe(CO)(CN)$_2$]		
CH_3OH		0.95[b]		
H_2O		1.07[b]		
		K[Cp*Fe(CO)(CN)$_2$]		
CH_3CN		0.36	89	0.78
		CpFe(CO)$_2$(CN)		
CH_3CN	−1.75			
		Cp*Fe(CO)$_2$(CN)		
CH_3CN	−1.92			

[a] All potential scaled to NHE referenced to a Cp_2Fe^+/Cp_2Fe standard ($E_{1/2}^{NHE}$ = 0.40 V) or a $MV^{2+}/MV^{+\bullet}$ standard ($E_{1/2}^{NHE}$ = −0.446 V).[12] A 2.5 mM analyte solution in CH_3CN or MeOH, 0.1 M TBAHFP electrolyte, measured vs $Ag/AgNO_3$ reference electrode. In H_2O solution, 0.1 M KCl supporting electrolyte, measured vs $Ag/AgNO_3$ reference electrode. [b] Irreversible cathodic potential. [c] Quasi-reversible reduction potential except where noted.

Fe(bipy)$_3^{2+/+}$ shows a more accessible $Fe^{II/I}$ couple at −1.18 V.[26] while a [Fe(CO)(N_HS_4-Et)]$^+$ complex, discussed further below, has a couple at −1.34 V.[27]

A substantial feature to the [CpFe(CO)(CN)$_2$]$^-$ and [Cp*Fe(CO)(CN)$_2$]$^-$ salts in organic solvents is a quasi-reversible anodic wave which is assigned to the $Fe^{II/III}$ couple as is consistent with assignments for Cp_2Fe (+0.40 V) and $[Fe(CN)_6]^{4-}$ (+0.356 V).[28] Increases in scan rate from 250 to 400 mV/s produce increases in the peak separation (ΔE_p) of the $Fe^{II/III}$ couple from 77 to 224 mV for K[CpFe(CO)(CN)$_2$] in CH_3CN, in agreement with the scan rate criterion for quasi-reversibility.[25] In aqueous solution, the anodic event for K[CpFe(CO)(CN)$_2$] is irreversible and at a quite high potential, +1.09 V; this suggests that the H-bonding that destabilizes the anion is detrimental to the oxidation process. In aqueous solution, the CV of the protonated form, H[CpFe(CO)(CN)$_2$], completely dissociated in water, is almost identical to that of K[CpFe(CO)(CN)$_2$]. Unfortunately, for comparison, the H[CpFe(CO)(CN)$_2$] is poorly soluble in CH_3CN. Other electrochemical measurements in protic solvents, i.e., MeOH, show cyclic voltammograms similar to those in CH_3CN within measurable solvent ranges, shifted positively by ca. 150 to 180 mV.

Electrochemical data of [Et_3NH][CpFe(CO)(CN)$_2$] in CH_3CN show a small positive shift (+20 mV) of the $Fe^{II/III}$ potential relative to K[CpFe(CO)(CN)$_2$] in CH_3CN; the small stabilization is presumed to be due to a weak hydrogen-bonding interaction between [Et_3NH]$^+$ counterion and CN^- ligands. Infrared spectroscopic results of [Et_3NH][CpFe(CO)(CN)$_2$] as compared to K[CpFe(CO)(CN)$_2$] also indicate that the H-bonding interac-

(24) Darensbourg, M. Y.; Barros, H. L. C. *Inorg. Chem.* **1979**, *11*, 3286.
(25) Bard, A. J.; Faulkner, L. R. In *Electrochemical Methods*; John Wiley & Sons: New York, 1980.
(26) Meites, L.; Zuman, P.; Narayanan, A. K.; Rupp, E. B. In *CRC Handbook Series in Inorganic Electrochemistry*; CRC Press: Boca Raton, FL,1983; Vol. III.
(27) Sellmann, D.; Becker, T.; Knoch, F. *Chem. Eur. J.* **1996**, *2*, 1092.
(28) Wilkinson, S. G.; Gillard, R. D.; McCleverty J. A. In *Comprehensive Coordination Chemistry*; Hawker, P. N., Twigg, M. V., Eds.; 1987, Vol. 4, p 1186.

Scheme 1[29]

$L_3Ru(PMe_3)_2CN + F_3CSO_3H \longrightarrow [L_3Ru(PMe_3)_2CNH][F_3CSO_3]$

	$-\Delta H_{CNH}$, Kcal/mol	ν(CN), cm^{-1}
L_3 = Cp*	25.0(2)	2057(m)
L_3 = Cp	22.4(2)	2065(m)

Scheme 2. $\Delta E(Fe^{III/II})$

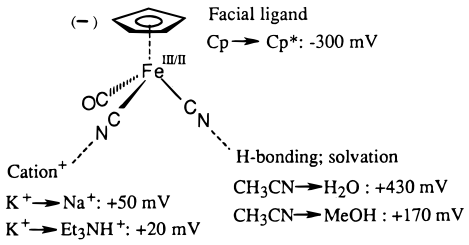

tions at CN^- implicated in the solid-state structure of the enzyme is present in CH_3CN solutions of the model complex.

For analogous ligand, solvent, and counterion environments, substitution of Cp for Cp* results in a −300-mV shift of the $Fe^{II/III}$ couple, in agreement with the negative shift in the irreversible cathodic event (presumably the $Fe^{II/I}$ reduction process) described above. Such results are consistent with thermochemical studies which quantitated the increase in basicity of the CN^- ligand in $CpRu(PR_3)_2CN$ vs $Cp^*Ru(PR_3)_2CN$.[29] For example, for R= Me, the data in Scheme 1 were reported. The thermochemical data agree with ν(CN) data in that the more exothermic protonation is at the CN^- of lower ν(CN), i.e., the more electron-rich Cp* derivative. Note that in this case a $\Delta\nu$(CN) of 8 cm^{-1} corresponds to a $\Delta(-\Delta H_{CNH})$ of 2.6 kcal/mol. Since the electronic communication from the facial ligand to the CN^- is via the metal center, we might expect even greater electron density differences to develop at the metal upon exchange of Cp to Cp* ligands. This change in the case of $CpFe(CO)(CN)_2^-$, vs $Cp^*Fe(CO)(CN)_2^-$, may be expressed in terms of the $Fe^{II/III}$ redox couples of 300 mV and relates to an average $\Delta\nu$(CN) of 10 cm^{-1}.

From Table 5, separations of the $Fe^{II/III}$ and $Fe^{II/I}$ potentials for the K^+ and Na^+ salts of $CpFe(CO)(CN)_2^-$ are computed to be 2.99 and 3.01 V, respectively. This separation is larger than that of the $[Fe(CO)(N_HS_4\text{-Et})]^+$ complex, 2.36 V, reported by Sellmann et al.[27] The electrochemical monitor of electronic changes at iron is summarized in Scheme 2 and expressed for the $Fe^{II/III}$ couple with $K[CpFe(CO)(CN)_2]$ in CH_3CN as the reference point; presumably the effects will be mirrored in the $Fe^{II/I}$ couple. *Clearly the internal coordination sphere donor change of Cp to Cp* has a major effect on electron density at iron in $L_3Fe(CO)(CN)_2^-$; solvation differences between H_2O and CH_3CN have an even larger effect.*

Although the electrochemistry of the neutral species is ill-behaved, cathodic peak potentials of $CpFe(CO)_2(CN)$ and $Cp^*Fe(CO)_2(CN)$ of −1.75 and −1.92 V, respectively, again display the destabilization of reduction by Cp*. Preliminary studies show that the irreversibilities (to be explored further in a separate study) are most probably due to the stabilization of Fe(I) by the two carbonyls leading to loss of the CN^- ligand and dimerization of the 17-electron radical, $CpFe(CO)_2^{\bullet}$. This reduction-promoted cyanide lability has precedence in studies of $[Fe^{II}(CN)_5(NO)]^{2-}$ which find that the one-electron reduced $[Fe(CN)_5(NO)]^{3-}$ species loses CN^- via a first-order process.[30]

(29) Nataro, C.; Chen, J.; Angelici, R. J. *Inorg. Chem.* **1998**, *37*, 1868.
(30) Nast, R.; Schmidt, J. *Z. Anog. Allg. Chem.* **1976**, *421*, 15.

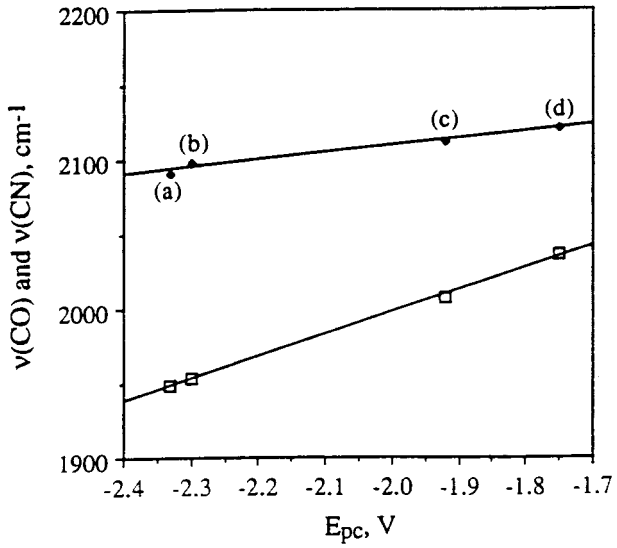

Figure 13. Correlation of average ν_{CO} vs E_{pc} (□) and average ν_{CN} vs E_{pc} (◆) for the various organometallic derivatives containing $Fe(CO)_x(CN)_y$ units (*data contained in Tables 1 and 5)*: (a) $[K][CpFe(CO)(CN)_2]$; (b) $[Na][CpFe(CO)(CN)_2]$; (c) $Cp^*Fe(CO)_2(CN)$; (d) $CpFe(CO)_2(CN)$.

Scheme 3[27,31]

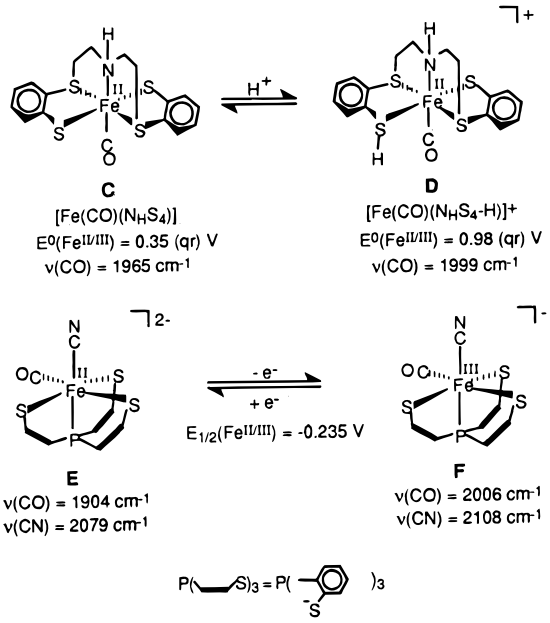

Assuming that the −1.75-V and −1.92-V E_{pc} values for $CpFe(CO)_2(CN)$ and $Cp^*Fe(CO)_2(CN)$ are indeed assignable to a one-electron reduction of Fe^{II} to Fe^{I}, respectively, these values along with the −2.33 and −2.30 V observed for the E_{pc} values of $K[CpFe(CO)(CN)_2]$ and $Na[CpFe(CO)(CN)_2]$, respectively, also show a linear correlation with average ν(CO) and ν(CN) (Figure 13). The more electron-rich systems as indicated by infrared spectroscopy are the more difficult to reduce. The slopes of the plots also show the responsiveness of the ν(CN) to electronic environment change is again about one-third that of the ν(CO).

Comparisons of Other Models. Two other model studies have been selected from the literature for comparison. Sellmann et al. have shown that protonation at one of thiolate ligands of the neutral iron(II) dithiolate monocarbonyl complex, $[Fe(CO)(N_HS_4)]$, represented as structures **C** and **D** in Scheme 3, results in a positive shift of the $Fe^{II/III}$ redox couple by +630 mV.[27]

This is similar to the difference between the E_{pc} values for the anionic dicyanide K[CpFe(CO)(CN)$_2$] and the neutral CpFe(CO)$_2$(CN) of ca. 580 mV and would appear to be mainly a charge effect. Koch and co-workers have noted a very accessible Fe$^{II/III}$ potential as indicated (referenced to NHE for comparison) in the tripodal phosphinotrithiolate cyanocarbonyl shown as structures **E** and **F**.[31] An interesting point is the +102 cm^{-1} shift in the ν(CO) value and +29 cm^{-1} shift in the ν(CN) that accompanies the Fe^{II} to Fe^{III} oxidation for **E** → **F**. A much smaller difference is occasioned on increase of positive charge via protonation of the thiolate ligand in Sellmann's complex, i.e., **C** → **D**.[27] In the latter case, the ν(CO) value of the Fe^{II} protonated form (ν(CO) = 1999 cm^{-1}) is shifted by + 34 cm^{-1} from that of the Fe^{II} neutral form (ν(CO) = 1965 cm^{-1}).

Comments and Conclusions

The study above is aimed at providing a reference point for the possible role(s) of the iron atom in the heterobimetallic active site of [NiFe]H$_2$ase, assuming the adjacent nickel site serves solely as a provider of metal−thiolate S-donor ligands to iron. We first comment on the well-known problem of the narrow biological redox range of [NiFe]H$_2$ase, i.e., −140 to −340 mV,[1,5,32] that encompasses the activation of the enzyme and presumably involves two oxidation state levels which were assigned to Ni$^{III/II}$ and Ni$^{II/I}$ couples before the heterobimetallic character of active site was discovered. Our work and the other two models for the iron site discussed above provide additional support for the thesis[26−28,31,33] that anionic thiolate ligands are required to bring the Fe$^{II/III}$ couple to within the biological range of [NiFe]H$_2$ase, and should this be achieved, the Fe$^{II/I}$ couple would be at best 2 V more negative. The best redox match is the Koch et al., anionic trithiolate.[31] However, it is evident that such an Fe$^{II/III}$ redox couple match produces a severe mismatch in vibrational spectroscopy of the reporter diatomics as the oxidation state of iron is changed between Fe^{II} and Fe^{III} and would create mismatches in both redox couple and vibrational spectroscopy if the oxidation state were changed by one unit lower, i.e., to Fe^{I}. The agreement in vibrational spectroscopy found for K[CpFe(CO)(CN)$_2$] and the oxidized enzyme produces a severe mismatch in redox potentials. We can only conclude from this dichotomy that the redox changes in [NiFe]H$_2$ase are not at iron in the active site of the enzyme, a conclusion consistent with other spectroscopies that find no evidence for a redox-active Fe pendant to Ni.[1]

The vibrational spectroscopy and electrochemical studies show the pyramidal fragment Fe(CO)(CN)$_2$ to sense electron density changes about the pseudo-octahedral model complex in a consistent and predictable manner. The well-known sensitivity of the ν(CO) frequency position to electronic changes at the metal center[34] is shown directly in the plot of redox potentials vs ν(CO) (Figure 13); that is, more electron-rich metals or complexes produce lower CO stretching frequencies consistent with π-back-bonding arguments. This correlation is mirrored by the ν(CN) in aprotic media, albeit in a less sensitive manner than ν(CO).

For the organometallic model, there is an excellent correlation between ν(CO) (or F_{CO}) and ν(CN) (or F_{CN}) that covers a broad range of electronic effects within a constant hexacoordinate structure and medium (CH$_3$CN). *When the shifts of ν(CO) and ν(CN) do not similarly respond, other factors are involved.* Notable are the deviations from this correlation both in the model and in the enzyme system (Figure 11). The enzyme states that are not in the catalytic cycle, i.e., in Figure 11 listed as (4), (5), (6), and (7) or Ni-Si$_{1934}$, Ni-B, Ni-A, and Ni-SU, respectively, reasonably fit the model complex correlation and are expected to maintain hexacoordination about iron. The active states, (1), (2), and (3) or Ni-Si$_{1914}$, Ni-R,and Ni-C, respectively, show large deviations from the linear plot of the model, as does the model system in aqueous solution. Established for the model system was the deviation produced by protic solvents, optimally solvating both CO and CN. Such H-bonding or protic solvation also has major effects on the relative intensities of ν(CO) and ν(CN) bands; these intensity ratio differences should similarly serve as sensors of such phenomena in the enzyme.

Scheme 4

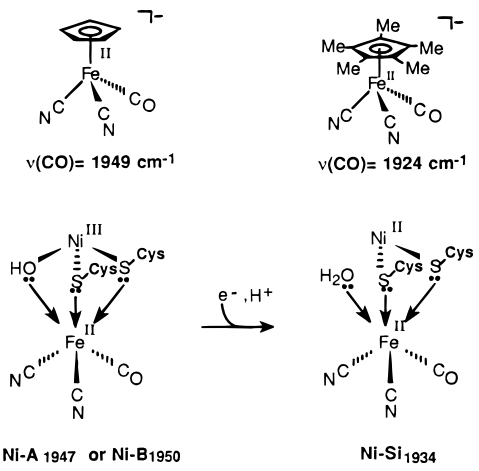

For the enzyme, several factors could produce the deviations from the ν(CO) vs ν(CN) plots, including coordination sphere/number changes, most notably the expected loss of the μ-oxo or μ-hydroxo bridging ligand as H$_2$O, producing a pentacoordinate species. Such a 16-electron Fe^{II} species might form an η^2-H$_2$ complex, perhaps commitant with a relative rotation of the pyramidal Fe(CO)(CN)$_2$ unit which could place both the CO and the CN in an H-bonding environment.

We are led to the inevitable conclusion that the Ni(μ-SCys)$_2$(μ-OH) donor set of Ni-A or Ni-B has the same electronic effect on the IR spectroscopic properties of the pyramidal Fe(CO)(CN)$_2$ fragment as does the 6-electron, symmetrical π-donor, C$_5$H$_5^-$. Since EPR measurements find an unpaired electron associated with nickel in these enzyme states, and reduction leads to an EPR silent state, at least one of the Ni−Si states, that with the 1934 cm^{-1} CO position, would appear to likewise contain a 6-electron facial donor set. The model mimics this conversion, producing a better electron donor to Fe(CO)(CN)$_2$, with the Cp → Cp* interchange (Scheme 4).

To make plausible proposals for the structures that are produced upon subsequent reductions (activation) of the enzyme necessitates considerations of iron-based vs nickel-thiolate-based H$_2$ reactivity. A minimal speculation would suggest that on further reduction, possibly of Ni^{II} to Ni^{I}, the μ-H$_2$O ligand is lost, producing a pentacoordinate (μ-Cys-S)$_2$Fe^{II}(CO)(CN)$_2$ species, i.e., the facial ligand set becomes a 4-electron donor, producing positive shifts in the diatomic vibrations. Uptake of H$_2$ at the open coordination site and subsequent heterolytic cleavage could reintroduce a hexacoordinate Fe^{II} hydride species of electronic character similar to that of the original μ-hydroxo species. Certainly such speculations are already in the literature

(31) Hsu, H.-F.; Koch, S. A.; Popescu, C. V.; Münck, E. *J. Am. Chem. Soc.* **1997**, *119*, 8371.
(32) Krüger, H.-J.; Peng, G.; Holm, R. H. *Inorg. Chem.* **1991**, *30*, 734.
(33) (a) Millar, M.; Lee, J. F.; Koch, S. A.; Fikar, R. *Inorg. Chem.* **1982**, *21*, 4105. (b) Sellmann, D.; Geck, M.; Moll, M. *J. Am. Chem. Soc.* **1991**, *113*, 5259.
(34) Tolman, C. A. *Chem. Rew.* **1977**, *77*, 313.

in various forms[4,35] and will remain speculations until an iron model with hydride or η^2-H_2 ligands is prepared.

Alternatively a Ni-SCys[36,37] or Ni-based mechanism for H_2 activation is attractive in that *cis*-Ni$(SCys)_2$ is at the entrance to the active site and S-based reactivity with small molecules is well established for nickel thiolates.[38] We have earlier suggested that interacting metal ions, producing heterobimetallics bridged by thiolates, should be useful for redox potential regulation, i.e., possibly providing an explanation for the narrow biological range of [NiFe]H_2ase.[39] In this view, the Fe(CO)-$(CN)_2$ unit is merely an auxiliary to the nickel ligands, providing a softer ligand set to facilitate Ni reduction.

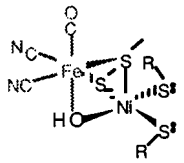

Thus, functional model studies continue to be a formidable and intriguing challenge to both synthetic[40] and theoretical chemists,[41] perhaps made less daunting by the well-developed field of diatomic vibrational spectroscopy.

Acknowledgment. Financial support was from the National Science Foundation (CHE 94-15901 to M.Y.D. and CHE 96-15866 to D.J.D.) for this work and CHE 85-13273 for the X-ray diffractometer and crystallographic computing system. Contributions from the R. A. Welch Foundation are also gratefully acknowledged. The pertinent coordinates for the [NiFe]H_2ase crystal structure were kindly made available to us by Drs. Michel Frey, A. Volbeda, and Juan Fontecilla-Camps, to whom we also acknowledge helpful discussion.

Supporting Information Available: Tables of crystallographic data collection parameters, atomic coordinates and equivalent isotropic displacement parameters, complete listings of bond lengths and bond angles, anisotropic displacement parameters, and observed and calculated ν(CO) and ν(CN) modes for isotopically labeled K[(η^5-C_5Me_5)Fe$(CN)_2$(CO)] derivatives; and packing diagrams for H[(η^5-C_5H_5)Fe$(CN)_2$(CO)] and K[(η^5-C_5Me_5)Fe$(CN)_2$(CO)]; (24 pages, print/PDF). A table of observed and calculated ν(CO) and ν(CN) modes for isotopically labeled K[(η^5-C_5Me_5)Fe$(CN)_2$(CO)] derivatives, and a description of the vibrational analysis (28 pages, print/PDF). See any current masthead page for ordering information and Web access instructions.

JA982053A

(35) Fontecilla-Camps, J. C. *Struct. Bonding* **1998**, *92*, 1 and references therein.

(36) Kumar, M.; Day, R. O.; Colpas, G. J.; Maroney, M. J. *J. Am. Chem. Soc.* **1989**, *111*, 5974.

(37) Roberts, L. M.; Lindahl, P. A. *Biochemistry* **1994**, *33*, 14339.

(38) Grapperhaus, C. A.; Darensbourg, M. Y. *Acc. Chem. Res.* **1998**, *31*, 451. Darensbourg, M. Y.; Tuntulani, T.; Reibenspies, J. H. *Inorg. Chem.* **1995**, *34*, 6287.

(39) Musie, G.; Farmer, P. J.; Tuntulani, T.; Reibenspies, J. H.; Darensbourg, M. Y. *Inorg. Chem.* **1996**, *35*, 2176.

(40) Shoner, S. C.; Olmstead, M. M.; Kovacs, J. A. *Inorg. Chem.* **1994**, *33*, 7. Hembree, R. T.; McQueen, J. S.; Day, V. W. *J. Am. Chem. Soc.* **1996**, *118*, 798. Marganian, C. A.; Vasir, H.; Baidya, N.; Olmstead, M. M.; Mascharak, P. K. *J. Am. Chem. Soc.* **1995**, *117*, 1584.

(41) Pavlov, M.; Siegbahn; P. E. M.; Blomberg, M. R. A.; Crabtree, R. H. *J. Am. Chem. Soc.* **1998**, *120*, 548.